

Cite this: *RSC Sustainability*, 2024, 2, 3298

## Fractional precipitation of Ni and Co double salts from lithium-ion battery leachates†

John R. Klaehn,<sup>1</sup> Meng Shi,<sup>1</sup> Luis A. Diaz,<sup>1</sup> Daniel E. Molina,<sup>1</sup> Reyixiati Repukaiti,<sup>1</sup> Fazlollah Madani Sani,<sup>2</sup> Margaret Lencka,<sup>2</sup> Andre Anderko,<sup>2</sup> Navamoney Arulsamy<sup>3</sup> and Tedd E. Lister<sup>1</sup>

Alternative sourcing of critical metals from lithium-ion batteries (LIBs) is necessary to secure the future supplies of Li, Ni, and Co. Most recovery processes of LIBs utilize pyrometallurgical and hydrometallurgical methodologies; however, these processes to recycle LIB cathode/anode materials can require several steps to isolate the desired metals. We have developed a facile isolation of the valued metals, where Ni and Co will co-crystallize as a sulfate double salt, called Tutton's salt  $[(\text{NH}_4)_2\text{Ni}/\text{Co}(\text{SO}_4)_2 \cdot 6\text{H}_2\text{O}]$ . Thermodynamic modelling of these Ni(II)/Co(II) sulfate double salts shows that Ni is less soluble than Co which could enhance the separation of Ni and Co from electrochemical (EC) leachates. This calculated difference between Ni and Co can be controlled further by temperature and ammonium sulfate concentration. Here, Ni-rich sulfate double salts were achieved at 30–45 °C while Co-rich sulfate double salts were formed at 2–9 °C, where 99% Ni and 89% Co were recovered from the EC-leach solution. Further tests with the leachate solution show that crystallization occurs above pH 2 which allows for higher pulp density leachates. Chemical analyses and single crystal X-ray characterization confirm that the Ni-rich sulfate double salts contain Ni and Co. However, the Co-rich sulfate double salts have ~30% Mn(II) in the crystal lattice with ~37% of Ni. As a result, this process reduces the total number of steps to isolate the desired metals while also reducing chemical waste generation and without employing organic solvents.

Received 12th June 2024  
Accepted 4th September 2024

DOI: 10.1039/d4su00303a

rsc.li/rscsus

### Sustainability spotlight

The world supplies of critical metals, such as nickel and cobalt, are strained in the areas that have these resources. In addition, end-of-life lithium-ion battery (LIB) components containing these critical metals are not easily recovered by traditional industrial extraction methods. We found that the addition of common chemical fertilizers will recover the nickel and cobalt from LIB leachate solutions. We report practicable methods for the isolation of materials that capitalizes on salting out the critical metal products as their Tutton's salts (sulfate double salts), which limits wastewater production, minimizes costly extraction processes, and possibly facilitates reprocessing them into battery cathodes. This article supports the following UN SDGs: responsible consumption and production, industry, innovation and infrastructure, and climate action.

## 1 Introduction

Sourcing critical metals (such as Li, Ni, Mn, and Co) for lithium-ion batteries (LIBs) is an important issue for the future electrification of small transportation as virgin materials are typically utilized in LIB manufacturing. End-of-life (EOL) LIBs offer the best alternative pathway for sourcing these critical metals.

Thus, establishing a circular economy for LIBs will become essential in addressing the shortfall in domestic metal supply and meeting world market demand.<sup>1,2</sup> However, the constant evolution of LIB cathode and anode formulations poses imminent problems which can complicate their recovery from spent materials. As a result, these evolving battery formulations introduce new complexities to metal separation processes. The simplification of the metal isolation steps is imperative to ensure the efficient recovery of these energy critical metals from spent LIBs.

LIB manufacturers require Ni and Co salts with high purity (e.g., >99 wt%) to create functional products. To be able to use recycled metals in new devices, extensive separation and recovery techniques are necessary to achieve the needed purity. However, high purity Ni and Co salts often require more isolation steps and create increasingly more waste by-products, both

<sup>1</sup>Critical Materials Innovation Hub, Idaho National Laboratory, 2525 Fremont Avenue, Idaho Falls, ID 83402, USA. E-mail: John.Klaehn@inl.gov

<sup>2</sup>Critical Materials Innovation Hub, OLI Systems Inc., 2 Gatehall Dr, Suite 1D, Parsippany, NJ 07054, USA

<sup>3</sup>University of Wyoming, 1000 E. University Ave., Laramie, WY 82071, USA

† Electronic supplementary information (ESI) available. CSD 2361136. For ESI and crystallographic data in CIF or other electronic format see DOI: <https://doi.org/10.1039/d4su00303a>



of which contribute to cost. To make LIB recycling economically viable and environmentally friendly, metal isolation with high purity needs to be performed with minimal steps.

For recovering valuable metals from EOL LIBs, they are initially converted into a black mass for recycling. The black mass is the main feedstock for hydrometallurgical or pyrometallurgical recycling processes.<sup>3</sup> Typically, the black mass is a crude mixture of valuable cathode metals (Li, Ni, Mn, and Co) along with impurities such as Fe, Al, Cu, and others. These impurities present a challenge in the efficient recovery of valuable metals from spent LIBs. Hydrometallurgical recycling of valuable metals from spent LIBs in the presence of impurities emerges as a feasible solution. However, the hydrometallurgical processes require excessive use of solvents, which generates chemical waste, posing economic and environmental challenges to the entire process.<sup>4–8</sup> Therefore, the current challenge in recycling spent LIBs through hydrometallurgical methods lies in identifying economic methodologies, particularly considering the tight cost margins in metal recovery yields.

A major problem in hydrometallurgical processing is high concentrations of Al and Fe that are typically found in LIB leachate.<sup>3,9–11</sup> At 3 wt% or higher concentrations, Al and Fe can reduce the effectiveness of common hydrometallurgical technologies, such as solvent extraction (SX) and ion exchange (IX), typically used to isolate the target metals. The most common method for removing metal ion impurities is aqueous base precipitation. For the case of Fe and Al impurities, the insoluble Fe and Al hydroxides are removed through filtration.<sup>3,9,10</sup> Moreover, it has been found that phosphate is an excellent choice for the precipitation of these metal ion impurities.<sup>12–14</sup> For our leachate solutions, we employed an electrochemical leaching (EC-leach) process that dissolved >99% of the metals in black mass and plated out copper on the cathode to create a copper-free LIB leachate.<sup>15</sup> Afterwards, we employed the phosphate precipitation technique for removing Al and Fe from a LIB leachate. During this process, ammonium phosphate can remove up to 99% of Fe and Al from the leachate solution.<sup>16</sup> The insoluble phosphate precipitate is readily separated by gravity or vacuum filtration, and the clean leachate solution can be utilized in other subsequent metal separation processes.

From our studies,<sup>16</sup> an unexpected result was found during our processing of the EC-leach solution, and a second precipitation (crystallization) of high purity Ni/Co sulfate double salt (Tutton's salt,  $(\text{NH}_4)_2\text{Ni}/\text{Co}(\text{SO}_4)_2 \cdot 6\text{H}_2\text{O}$ ) was recovered. The X-ray diffraction (XRD) and atomic absorption spectroscopic (AAS) analyses showed that the chemical structure of the Ni/Co solid solution was  $(\text{NH}_4)_{2.78}\text{Ni}_{0.78}\text{Co}_{0.22}(\text{SO}_4)_2 \cdot 6\text{H}_2\text{O}$ . It is notable that our EC-leachates contained a mixed metal solution with phosphates and sulfates that resulted in a two-step precipitation process that removes impurity metals and yields a Ni/Co sulfate double salt for recovery. These two precipitation processes occur at different temperatures, but the sulfate double salt showed an opportunity to isolate Ni and Co from the same leachate with minimal effort. Literature does not show this two-step process; however, it is known that the ammonium sulfate double salts can be formed upon cooling or evaporation if there is excess ammonium ion. Generally, in most metal

recovery methods, ammonium sulfate double salts are undesirable due to the presence of two or more metals that can interfere with concurrent solvent separation methodologies that favor single metal extraction. From this finding, it is suggested that formation of ammonium sulfate double salt can facilitate quick and effective recovery of Co and Ni from a leachate. In this article, we show an improved isolation method with a high recovery of Ni/Co sulfate double salts from our LIB EC-leachates, with supporting thermodynamic modeling of these double salts.

## 2 Experimental

### 2.1 Materials

Surrogate leachate solutions were prepared with lithium sulfate monohydrate ( $\text{Li}_2\text{SO}_4 \cdot \text{H}_2\text{O}$ , Alfa Aesar, 99%), manganese(II) sulfate monohydrate ( $\text{MnSO}_4 \cdot \text{H}_2\text{O}$ , Alfa Aesar, 99%), nickel(II) sulfate hexahydrate ( $\text{NiSO}_4 \cdot 6\text{H}_2\text{O}$ , Fisher Scientific, >95 wt%), cobalt(II) sulfate heptahydrate ( $\text{CoSO}_4 \cdot 7\text{H}_2\text{O}$ , Ward's Science, >99%), and sulfuric acid ( $\text{H}_2\text{SO}_4$ , Fisher Scientific, 95–98 wt%). Ammonium sulfate ( $(\text{NH}_4)_2\text{SO}_4$ , ACROS Organics, ACS, 99+%), ammonium hydroxide ( $\text{NH}_4\text{OH}$ , Fisher Scientific, 30–33 wt% (aq.)), and diammonium hydrogen phosphate (DAP,  $(\text{NH}_4)_2\text{HPO}_4$ , Sigma Aldrich, 99%) were also employed in crystallization procedures. Chemicals were used without further purification. Nano-pure water used in this study was obtained from a PURELAB Flex 1 (18.2 MΩ cm). Lithium-ion battery black mass (LIBBM) was obtained from Retrie Technologies (now Cirba Solutions).

### 2.2 Tutton's salts crystallization

**2.2.1 Formation of Tutton's salts.** Tutton's salt crystallization was observed after employing a previously published EC-Leach process<sup>15</sup> using LIBBM feedstock. Metals of interest (Li, Mn, Co, and Ni) and impurity metals (Al, Fe, and Zn) were contained in the leachate solution at a final pH between 1 and 2. The results of this study showed that the impurity metals prevented further metal separation, particularly when their concentrations were high (>3 wt%). From a previous published process,<sup>16</sup> these impurities were removed by adding diammonium phosphate (DAP). This was done by slowly raising the pH to 3–4 with a mL of 30–33 wt%  $\text{NH}_4\text{OH}$ , while keeping the temperature at 45–50 °C. As a result, precipitation occurred which was found to be a mixture of Al, Fe and Zn phosphates. The phosphate precipitates were filtered from the warm solution. The clean leachate solution having the remaining metals, mainly Ni, Co, Li, and Mn, was left to cool to room temperature. After 2–3 days, it was observed that Ni/Co double sulfate salts precipitated from the solution as large green crystals. The crystals were easily recovered by decanting the remaining solution. It should be noted that the solution pH did not change after crystal deposition.

**2.2.2 Tutton's salts from simulated solutions: crystallization tests.** To study the formation of the Tutton's salts, several surrogate tests were conducted.  $\text{NiSO}_4 \cdot 6\text{H}_2\text{O}$ ,  $\text{CoSO}_4 \cdot 7\text{H}_2\text{O}$ ,  $\text{MnSO}_4 \cdot \text{H}_2\text{O}$  and  $\text{Li}_2\text{SO}_4 \cdot \text{H}_2\text{O}$  were mixed with diluted 0.01 M



H<sub>2</sub>SO<sub>4</sub> to simulate the clean leachates, with Li concentration 6 g L<sup>-1</sup>, Mn concentration 4 g L<sup>-1</sup>, and a combination of Ni and Co at 40 g L<sup>-1</sup> (total metal concentration). Ni : Co weight ratios were 100 : 0, 90 : 10, 80 : 20, 70 : 30, 60 : 40, 50 : 50, 40 : 60, 30 : 70, 20 : 80, 10 : 90, and 0 : 100. In addition, DAP and NH<sub>4</sub>OH were added to simulate the processed EC-Leach solutions after the precipitation of the phosphate impurity metals.<sup>16</sup> The pH values of the surrogate solutions were adjusted with DAP to 3, and then with 30–33 wt% NH<sub>4</sub>OH to reach pH of 4. After heating the mixture at 40–50 °C, 2 M (NH<sub>4</sub>)<sub>2</sub>SO<sub>4</sub> was added to reach 1 or 1.5 molar equivalents to the total moles of Ni and Co. The obtained solutions were left overnight at room temperature or in a fridge (9 °C).

**2.2.3 Tutton's salts formation from real processed leachates.** To accelerate the Tutton's salt formation, a clean leachate (1.7 L, ~71 g L<sup>-1</sup> total metals) was heated to 70 °C, and 283 g (NH<sub>4</sub>)<sub>2</sub>SO<sub>4</sub> was added at 1.5 times of the total moles of Ni and Co (~46 g L<sup>-1</sup>). Crystals formed quickly and were removed *via* filtration when the solution was warm. Then the liquid phase was transferred to a fridge (9 °C) overnight. More crystals were generated and were separated through vacuum filtration (See ESI S1†).

Leachates, DAP precipitates, clean leachate, Tutton's salt crystals and filtrates were sampled for metal composition analysis.

### 2.3 Characterization

Atomic Absorption Spectroscopy (AAS, Agilent, 240FS AA) was used to measure metal concentrations. The equipment was calibrated using commercially available standard solutions (1000 µg mL<sup>-1</sup>, Agilent). Metal concentrations in the prepared calibration standard were 1 mg L<sup>-1</sup> for Cd and Zn, 40 mg L<sup>-1</sup> for Al, and 5 mg L<sup>-1</sup> for Ni, Co, Li, Mn, Fe, and Cu. Solid samples were dissolved in concentrated hydrochloric acid (HCl, Fisher Chemical™, Certified ACS Plus, 36.5 to 38.0 wt%). Liquid samples, including clean leachates, filtrates, and dissolved solids, were diluted with 3 wt% HCl to the target concentrations.

XRD patterns for the Tutton's salt were measured at 150 K on a Bruker SMART APEX II CCD area detector system equipped with a graphite monochromator and a Mo K $\alpha$  fine-focus sealed tube operated at 1.5 kW power (50 kV, 30 mA). The crystals were mounted on a glass fiber using Paratone N oil and the detector was placed at 5.13 cm from the crystal during the data collection. A series of narrow frames of data were collected with a scan width of 0.5 in  $\omega$  or  $\phi$  and an exposure time of 20 s per frame. The frames were integrated with the Bruker SAINT software package using a narrow-frame integration algorithm. The data were corrected for absorption effects by the multi-scan method (SADABS). Crystallographic data collection parameters and refinement data are collected below in Table 1. Structures were solved by the direct methods using the Bruker SHELXTL software package.<sup>17</sup>

### 2.4 Thermodynamic modelling

To elucidate the conditions that are conducive to the formation of the Tutton's salt from the leachate solution,

**Table 1** Crystal data and structure refinement for (NH<sub>4</sub>)<sub>2</sub>Ni<sub>0.78</sub>Co<sub>0.22</sub>(H<sub>2</sub>O)<sub>6</sub>(SO<sub>4</sub>)<sub>2</sub>

Identification code	jrk06a	
Empirical formula	(Co <sub>0.22</sub> /Ni <sub>0.78</sub> )N <sub>2</sub> H <sub>20</sub> O <sub>14</sub> S <sub>2</sub>	
Formula weight	395.06	
Temperature	150(2) K	
Wavelength	0.71073 Å	
Crystal system	Monoclinic	
Space group	P2 <sub>1</sub> /c	
Unit cell dimensions	$a = 6.2541(4)$ Å	$a = 90^\circ$
	$b = 12.3277(8)$ Å	$b = 107.006(2)^\circ$
	$c = 9.1119(6)$ Å	$g = 90^\circ$
Volume	$671.80(8)$ Å <sup>3</sup>	
Z	2	
Density (calculated)	1.953 g cm <sup>-3</sup>	
Absorption coefficient	1.792 mm <sup>-1</sup>	
F(000)	412	
Crystal size	0.437 × 0.304 × 0.262 mm <sup>3</sup>	
Theta range for data collection	2.863 to 36.445°	
Index ranges	-10 ≤ $h$ ≤ 10, -20 ≤ $k$ ≤ 20, -15 ≤ $l$ ≤ 15	
Reflections collected	25 862	
Independent reflections	3272 [ $R(\text{int}) = 0.0244$ ]	
Completeness to theta = 25.242°	98.90%	
Absorption correction	Multi-scan	
Max. and min. transmission	0.7471 and 0.6270	
Refinement method	Full-matrix least-squares on F <sub>2</sub>	
Data/restraints/parameters	3272/0/130	
Goodness-of-fit on F <sub>2</sub>	1.093	
Final $R$ indices [ $I > 2\sigma(I)$ ]	$R1 = 0.0168$ , $wR2 = 0.0425$	
$R$ indices (all data)	$R1 = 0.0184$ , $wR2 = 0.0431$	
Extinction coefficient	n/a	
Largest diff. peak and hole	0.442 and -0.493e Å <sup>-3</sup>	

a thermodynamic model has been constructed using the Mixed-Solvent Electrolyte (MSE) framework.<sup>18,19</sup> The MSE framework is suitable for this purpose because it is capable of reproducing the thermophysical properties of multicomponent salt solutions ranging from infinite dilute to very concentrated (*i.e.*, up to the saturation limit) over wide ranges of temperatures and pressures. The MSE model combines an equation of state for standard-state properties of individual species, an excess Gibbs energy model to account for non-ideal behavior of the chemical system, and an algorithm for simultaneously solving chemical and phase equilibria. This makes it possible to reproduce speciation-based properties such as equilibrium concentrations of species, their activity coefficients, and autogenous pH of solution in addition to phase equilibria. The MSE model is parameterized using a bottom-up approach, *i.e.*, by developing model parameters for constituent simple subsystems (primarily binary mixtures) followed by more complex ternary and higher-order systems. The parameters are regressed using multiple properties (such as solid solubilities, vapor–liquid equilibria, osmotic and activity coefficients, heats of mixing and dilution, and heat capacities) as described previously.<sup>18,19</sup> In previous studies, the MSE model has been shown to accurately reproduce solubilities in multicomponent systems containing various classes of salts, *e.g.*, those of alkali and alkaline earth metals,<sup>20</sup> rare earth elements,<sup>21,22</sup> actinides<sup>23</sup> and transition metals.<sup>24</sup> In this study, we extend the MSE model to mixtures that combine Ni, Co, Mn, and Li sulfates with ammonium sulfate. After



verifying the accuracy of the model for the relevant ternary systems (*i.e.*,  $\text{NiSO}_4\text{--}(\text{NH}_4)_2\text{SO}_4\text{--H}_2\text{O}$ ,  $\text{CoSO}_4\text{--}(\text{NH}_4)_2\text{SO}_4\text{--H}_2\text{O}$ ,  $\text{MnSO}_4\text{--}(\text{NH}_4)_2\text{SO}_4\text{--H}_2\text{O}$ , and  $\text{Li}_2\text{SO}_4\text{--}(\text{NH}_4)_2\text{SO}_4\text{--H}_2\text{O}$ ), we apply the model to multiple cation/anion mixtures containing both nickel and cobalt. ESI S2† describes the validation of the model for these systems using solubility data that have been reported in the literature.

### 3 Results and discussion

#### 3.1 Sulfate double salt (Tutton's salt) formation from EC-leachate

From our previous report, the EC-leach process liberated valuable metals (Li, Co, Mn and Ni) into a leachate solution.<sup>15</sup> However, impurity metals (such as Al and Fe) proved troublesome for further metal isolation, but these impurities could be removed by increasing the solution pH with DAP. The Al and Fe phosphate precipitates were subsequently filtered from the warmed EC-leachate. Once the filtrate was allowed to cool to room temperature under ambient conditions, precipitates formed that were identified as Ni(II)/Co(II) sulfate double metal salts, or Tutton's salts. Interestingly, the same EC-leachate solution encouraged the formation of Tutton's salts, indicating that enough ammonium existed for the growth of Tutton's salts.

Tutton's salts are well-documented in literature, and their crystal structure suggests that they generally form as the metal sulfate double salt hexahydrate,  $(\text{NH}_4)_2\text{M}(\text{SO}_4)_2 \cdot 6\text{H}_2\text{O}$  [M = divalent metal (transitional elements) ions].<sup>25–30</sup> The conventional method to form a mixed Ni/Co Tutton's salts is by mixing  $(\text{NH}_4)_2\text{SO}_4$  with a Ni(II) and Co(II) mixed sulfate solution. In eqn (1), the reaction of these Ni/Co sulfate double salts with  $(\text{NH}_4)_2\text{SO}_4$  are shown, especially for processing in Cu-free leachate solutions.



In our Cu-free, EC-leachate,<sup>16</sup> green Tutton's salt crystals readily formed in solution with a preference of Ni(II) and Co(II) in a fixed stoichiometry crystal lattice. Even though Ni and Co dominated the crystal structure, roughly 2 wt% Mn(II) was detected by AAS in these crystals. In addition, Cu(II), Fe(II), or Zn(II) can co-crystallize with Ni(II) and Co(II) if they exist in solution. Spent LIB leachates obtained *via* our EC-Leach and phosphate precipitation allow low to no interference ions of Cu(II), Fe(II), and Zn(II) in the downstream processing. For the sulfate double salt process, most literature reports utilize simulated solutions of LIB leachates excluding the noted interference metals Al, Fe, and Cu.<sup>26,31</sup> With our processing methods, Tutton's salt formation proves to be a practical pathway for purification of Ni/Co from nickel–manganese–cobalt (NMC) cathodes. The current economic driver for NMC is the isolation of Ni and Co from recycled NMC leachate solutions, which is challenging by using SX, IX or other precipitation pathways.

Fig. 1 shows a single crystal X-ray structure of the isolated Tutton's salt and its green salt crystals from a processed EC-leach solution (no Cu, Fe, Al, or Zn). The AAS results of the green crystals revealed a metal composition of Ni(II) and Co(II) in a ratio of 0.78 : 0.22, respectively. This chemical composition used in the X-ray determination identified the crystal as a Tutton's salt structure  $(\text{NH}_4)_2[\text{Ni}_{0.78}\text{Co}_{0.22}(\text{H}_2\text{O})_6](\text{SO}_4)_2 \cdot 1$ .<sup>26,31</sup> By adjusting the X-ray data to accommodate the specific percentage of Ni and Co in the lattice, the crystal structure was refined to a high degree of confidence with an  $[I > 2\delta(I)]$  of  $R1 = 0.0168$ ,  $wR2 = 0.0425$ . These data indicate a monoclinic crystal system, featuring ammonium and sulfate in the crystal lattice with nearby Ni and Co ions. The presence of water is confirmed

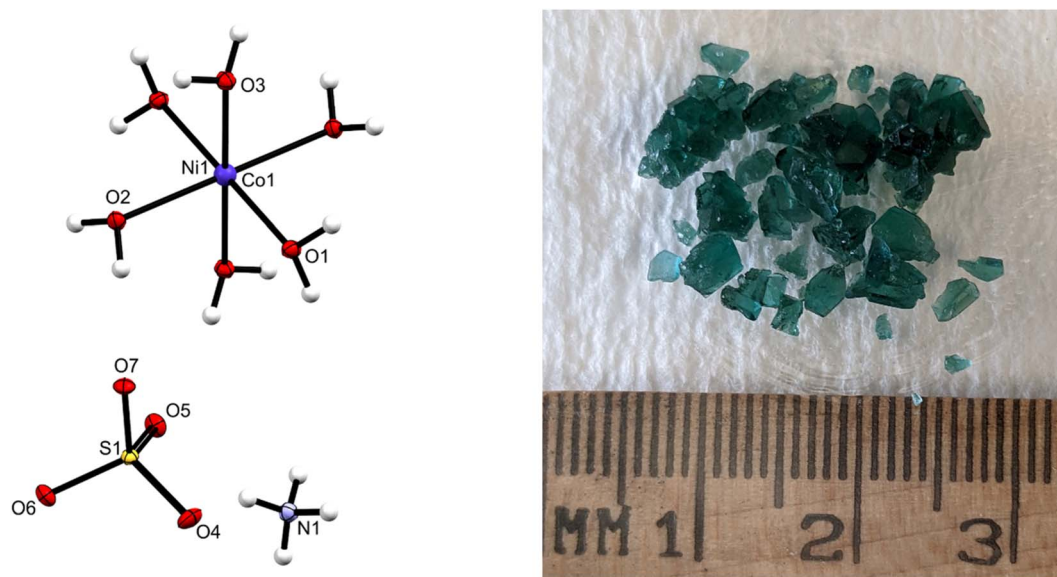


Fig. 1 (Left) View of the  $[\text{Ni}_{0.78}/\text{Co}_{0.22}(\text{H}_2\text{O})_6]^{2+}$ ,  $\text{SO}_4^{2-}$  and  $\text{NH}_4^+$  cation in **1**. The central atom in the complex cation is labeled as both Ni and Co atoms as the site is shared by the two atoms. The thermal ellipsoids are drawn at 50% probability. The three symmetrically equivalent O atoms and all H atoms are unlabeled and (Right) isolated Tutton's salt crystals.



as a hexa-hydrate. The resulting Tutton's salt crystal has similar bond angles and bond distances consistent with those in literature.<sup>26,31</sup> In Table 1, some of the crystallographic data and refinement parameters, as well as other relevant crystallographic data are given for **1** (see ESI S3,† CSD 2361136 contains the supplementary crystallographic data for this paper.). In the identified structure, sulfate and ammonium are near each other, suggesting some bonding with the water molecules on the metal. The octahedral formation of the water molecules around the nickel has slightly altered angles from the ideal 90°, which however is attributed to the Jahn–Teller effect impacting the crystal packing. In summary, the crystallographic data are consistent with the proposed structure of the Tutton's salt presented in this work.

### 3.2 Fractional crystallization of sulfate double salts (Tutton's salt) from EC-leachate

Fractional precipitation (or fractional crystallization) methods of metals are commonly used in industrial applications for product purification and waste treatment using chemical, temperature, and/or pressure methodologies.<sup>32–34</sup> Furthermore, fractional precipitation is generally the lowest energy consuming separation process(es); however, the time necessary to recover target metals can vary greatly depending on the chemistry and the product purity. For recycling, the isolation of Ni and Co from a black mass leachate is dependent on the impurity metals. For most leachates, removal of impurity metals is required for the target metals. In our example, DAP addition quickly precipitated the impurity metals as their phosphates,<sup>16</sup> and then followed by a second precipitation of the sulfate double salts that was rich in Ni and Co. In Table 2, the metal sulfates show some different solubilities; however, the double salt with ammonium has dramatically less solubility in comparison.

In Table 2, variation in solubility of the metal sulfates show some interesting trends. The hydrated metal sulfates (left column, Table 2) show very good solubility, which indicates that alternative separation methodologies, such as IX or SX, are necessary to recover most of these metals from solution. Most industrial processes focusing on metal sulfate isolation through precipitation require either water evaporation or high concentrations of sulfate salts. Here, the difference between the solubility of Ni and Co/Mn sulfate salts are large enough to separate Ni, but the separation of Co and Mn requires IX or SX. On the

other hand, ammonium sulfate double salts (right column, Table 2) show much lower solubility values compared to the metal sulfates, which makes them good candidates for precipitation or crystallization methods. The solubility of Ni Tutton's salt is the lowest, where Co is nearly twice Ni's solubility. However, the solubility of Mn Tutton's salt is much higher than for Ni or Co. This solubility data indicates that these metals have the potential to be isolated individually from the processed EC-leachate solutions in the form of their Tutton's salts. From Table 1 and Fig. 1, a high percentage of Ni with some Co was found in **1**, and the Mn was greatly diminished. This observation indicates that the double salt precipitation or crystallization process can control the recovery of the valuable metals of Co and Ni from EC-leachate containing NMC. Also, it suggests that fewer processing steps are needed to recover high percentages of Ni and Co, compared to SX and IX.

To explain the observed crystallization of **1** from EC-leachate, Table 3 shows the metal composition of the black mass where 99% of the metals is dissolved, and then its EC-leachate after impurity removal of Fe/Al.<sup>16</sup> Afterwards, the remaining EC-leachate had extremely low concentration of Fe and Al ions, but the solution had an excess of ammonium cations, due to the final pH adjustment with NH<sub>4</sub>OH. In our previous study, ammonium was the limiting reagent, assuming sulfate was a large excess in the EC-leachate. To achieve a Tutton's salt, the chemical stoichiometry requires two sulfates and two ammoniums for each metal ion. From our previous report,<sup>16</sup> **1** has a low solubility in the EC-leachate solution from Table 3, and the formation of **1** is favored in this EC-leachate when containing a sufficient quantity of ammonium and sulfate.

### 3.3 Thermodynamic modelling on double sulfate salts (Tutton's salts)

Since ammonium is clearly influencing the double sulfate salt (Tutton's salt) formation, the relationship between phosphate and sulfate precipitations cannot be easily explained. The solubility differences between phosphate and sulfate would seem to favor metal phosphate precipitation over metal sulfate precipitation.<sup>35</sup> However, introducing ammonium changes the kinetics of the precipitation reactions, which allows Fe and Al to precipitate quickly and then the Ni/Co Tutton's salt to crystallize later. The question is how pH, ion concentrations, and temperature affect the chemistry of these systems (eqn (1)). To elucidate these effects, thermodynamic modelling can evaluate

Table 2 Equilibrium solubility of sulfate salts (kg of salt per kg of water) in water at 25 °C

Sulfate	Solubility (kg/kg water)	Ammonium sulfate	Solubility (kg/kg water)
NiSO <sub>4</sub> ·6H <sub>2</sub> O	0.530 <sup>a</sup>	(NH <sub>4</sub> ) <sub>2</sub> Ni(SO <sub>4</sub> ) <sub>2</sub> ·6H <sub>2</sub> O	0.075 <sup>d</sup>
CoSO <sub>4</sub> ·7H <sub>2</sub> O	0.604 <sup>b</sup>	(NH <sub>4</sub> ) <sub>2</sub> Co(SO <sub>4</sub> ) <sub>2</sub> ·6H <sub>2</sub> O	0.147 <sup>e</sup>
MnSO <sub>4</sub> ·H <sub>2</sub> O	0.643 <sup>c</sup>	(NH <sub>4</sub> ) <sub>2</sub> Mn(SO <sub>4</sub> ) <sub>2</sub> ·6H <sub>2</sub> O	0.372 <sup>e</sup>

<sup>a</sup> Janssen I. B., *et al.*, 2021, *Crystals*, **11**, 1485. <sup>b</sup> Kim J. H., *et al.*, *Cobalt and Inorganic Cobalt Compounds*, World Health Organization, 2006. <sup>c</sup> Maeda K., *et al.*, *Developments in Chemical Engineering and Mineral Processing*, 2003, **11**, 423–435. <sup>d</sup> Mullin J. W. and Osman M. M., *J. Chem. Eng. Data*, 1967, **12**, 516–517. <sup>e</sup> Seidell A., *Solubilities of Inorganic and Organic Substances: A Compilation of Quantitative Solubility Data from Periodical Literature*, D. Van Nostrand Company, 1919.



Table 3 Metal composition of black mass and EC-leachate sulfate that gave Tutton's salt, 1

Composition	Ni <sup>2+</sup>	Co <sup>2+</sup>	Li <sup>+</sup>	Mn <sup>2+</sup>	Al <sup>3+</sup>	Fe <sup>3+</sup>	Cu <sup>2+</sup>	Zn <sup>2+</sup>	Total
Black mass (wt%)	15.70	6.5	3.15	2.00	0.65	0.30	0.40	0.01	
EC-leach solution (g L <sup>-1</sup> )	30.86	15.07	5.54	3.72	1.29	0.53	0.12	0.02	
EC-leach solution (mol L <sup>-1</sup> )	0.526	0.256	0.80	0.067	0.048	0.010	0.002	0.0003	1.707

the described Ni/Co sulfate double salt formation through a comparison of (NH<sub>4</sub>)<sub>2</sub>Ni(SO<sub>4</sub>)<sub>2</sub> and (NH<sub>4</sub>)<sub>2</sub>Co(SO<sub>4</sub>)<sub>2</sub> solubilities in aqueous solutions.

Fig. 2 compares the effect of temperature on solubility of ammonium cobalt sulfate, ammonium nickel sulfate, and Ni/Co sulfate double salt hexahydrates (Tutton's salt). The data was simulated on the parent Ni and Co sulfate double salts by utilizing their molal solubility (mol salt per kg water) at different temperatures. In Fig. 2, the experimental solubility data are only shown for (NH<sub>4</sub>)<sub>2</sub>Co(SO<sub>4</sub>)<sub>2</sub>·6H<sub>2</sub>O, and the (NH<sub>4</sub>)<sub>2</sub>Ni(SO<sub>4</sub>)<sub>2</sub>·6H<sub>2</sub>O data is given in ESI S2.† Overall, the stoichiometric coefficients of Ni and Co in these three hydrates are different and, therefore, their solubility values at a constant temperature cannot be used as a reference for identifying which Ni/Co composition is favored.

From Fig. 2, solubility of all three hydrates increases with increasing solution temperature. The increasing trend in solubility of the Ni/Co sulfate double salt hydrates explains the observations reported previously.<sup>27,30,36–50</sup> In the temperature range from 25 °C to 50 °C, the solubilities of (NH<sub>4</sub>)<sub>2</sub>Ni(SO<sub>4</sub>)<sub>2</sub>·6H<sub>2</sub>O and Ni/Co double salt are closely related, while the solubility of (NH<sub>4</sub>)<sub>2</sub>Co(SO<sub>4</sub>)<sub>2</sub>·6H<sub>2</sub>O is nearly twice as high. Heating up the solution to 40–50 °C increases Ni/Co Tutton's salt solubility while facilitating the precipitation of Al and Fe phosphates. When the solution temperature decreases to room temperature, solubility of the Ni/Co Tutton's salt decreases, and the solution becomes supersaturated and then the Ni/Co green crystals form.

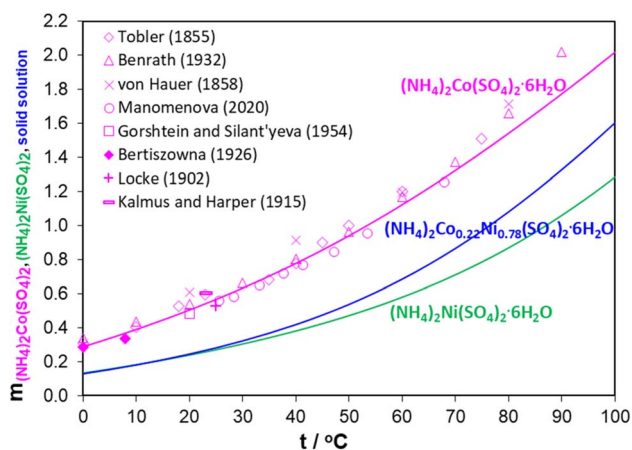


Fig. 2 Literature and calculated solubility of (NH<sub>4</sub>)<sub>2</sub>Co(SO<sub>4</sub>)<sub>2</sub>·6H<sub>2</sub>O, (NH<sub>4</sub>)<sub>2</sub>Ni(SO<sub>4</sub>)<sub>2</sub>·6H<sub>2</sub>O, and isolated Ni/Co Tutton's salt ((NH<sub>4</sub>)<sub>2</sub>Co<sub>0.22</sub>Ni<sub>0.78</sub>(SO<sub>4</sub>)<sub>2</sub>·6H<sub>2</sub>O) in water as a function of solution temperature. Y-axis unit: mol salt per kg water.

Fig. 3 presents the variations in the calculated solubility values of the three hydrates as a function of solution pH at 9 °C, 25 °C, and 50 °C. H<sub>2</sub>SO<sub>4</sub> and NH<sub>4</sub>OH were used in the simulations as the pH-adjusting agents. It shows that at pH 1 to 6, the solubility of the three salts becomes smaller in the following order: (NH<sub>4</sub>)<sub>2</sub>Co(SO<sub>4</sub>)<sub>2</sub>·6H<sub>2</sub>O > Ni/Co Tutton's salt > (NH<sub>4</sub>)<sub>2</sub>Ni(SO<sub>4</sub>)<sub>2</sub>·6H<sub>2</sub>O. The main conclusion is that a change in solution pH barely influences the solubility of three salts in a practically relevant pH range. This agrees with a previous report<sup>28</sup> that low pH (pH 1–5) does not affect the crystallization behavior of these double salts, which can isolate Ni/Co from the leachate without having to increase pH. This means that the addition of DAP to the solution caused an increase in solution pH to 3–4 but did not impact the solubility of these three Tutton's salts. At pH 2 or lower, the acid dissociation of bisulfate (pK<sub>a</sub> = 1.99) becomes a factor, which decreases double salt formation and its subsequent precipitation from solution. However, pH certainly influences the solubility of the Al and Fe phosphate salts due to their solubility limits at a low pH range. It was observed that pH of the leachate solution did not change after the Ni/Co Tutton's salt crystallization. This aligns with the observation that the solubility of the Ni/Co Tutton's salt is independent of the solution pH, as demonstrated by the simulations in Fig. 3.

Fig. 4 shows the changes in the calculated solubility values of (NH<sub>4</sub>)<sub>2</sub>Co(SO<sub>4</sub>)<sub>2</sub>·6H<sub>2</sub>O, (NH<sub>4</sub>)<sub>2</sub>Ni(SO<sub>4</sub>)<sub>2</sub>·6H<sub>2</sub>O, and the Ni/Co Tutton's salt, respectively, as a function of (NH<sub>4</sub>)<sub>2</sub>SO<sub>4</sub> concentration at 9 °C, 25 °C, and 50 °C. The vertical dashed lines are the practical maximum limits of (NH<sub>4</sub>)<sub>2</sub>SO<sub>4</sub> that can be added to the solution and promote the crystallization of these hexahydrates.

The solubility of all three hydrate crystals decreases dramatically with increasing (NH<sub>4</sub>)<sub>2</sub>SO<sub>4</sub> concentrations. The comparison of the Ni/Co Tutton's salt crystallization in the EC-leachate and surrogate solutions showed that the Ni/Co Tutton's salt forms in the EC-leachate solutions but not the surrogate solutions. The simulations given in Fig. 4 support the hypothesis that at low (NH<sub>4</sub>)<sub>2</sub>SO<sub>4</sub> concentrations (resembling the surrogate solutions), the Ni/Co Tutton's salt solubility remains high, *i.e.*, the solution is undersaturated with respect to the Ni/Co Tutton's salt, and therefore, it does not precipitate. At higher (NH<sub>4</sub>)<sub>2</sub>SO<sub>4</sub> concentrations (resembling the EC-leachate solution), the solubility of the Ni/Co Tutton's salt is small, which means that the leachate solution can easily become supersaturated, and crystallization of the Ni/Co Tutton's salt occurs.

Double salt formation with surrogate solutions containing Ni and Co has been investigated previously; however, they did not contain Cu, Fe, or Al, which favors double salt formation



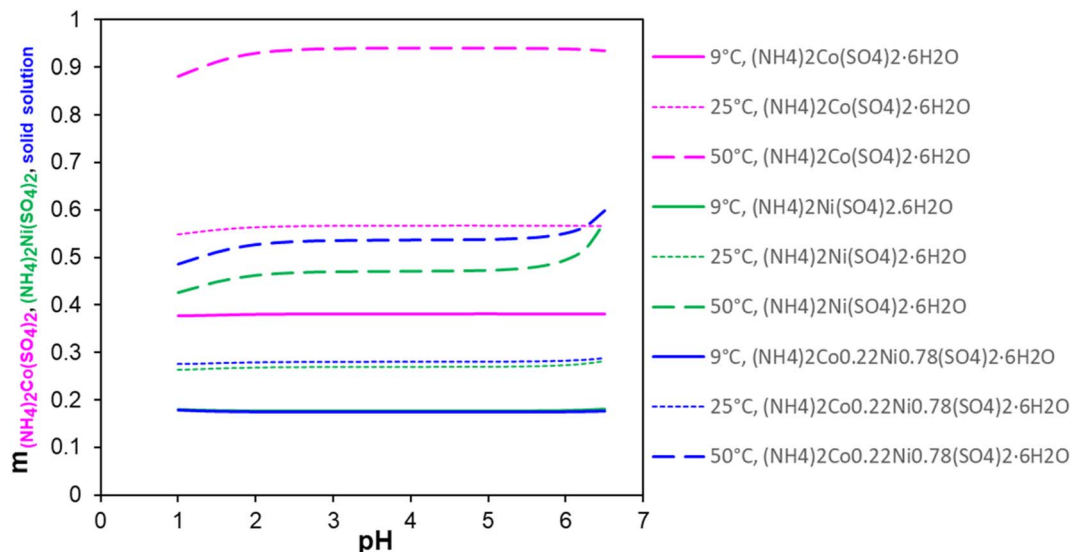


Fig. 3 Variations in the calculated solubilities of  $(\text{NH}_4)_2\text{Co}(\text{SO}_4)_2 \cdot 6\text{H}_2\text{O}$ ,  $(\text{NH}_4)_2\text{Ni}(\text{SO}_4)_2 \cdot 6\text{H}_2\text{O}$ , and Ni/Co Tutton's salt (referred to as solid solution, isolated  $(\text{NH}_4)_2\text{Co}_{0.22}\text{Ni}_{0.78}(\text{SO}_4)_2 \cdot 6\text{H}_2\text{O}$ ) in water as a function of solution pH at 9 °C, 25 °C and 50 °C. Y-axis unit: mol salt per kg water.

upon addition of  $(\text{NH}_4)_2\text{SO}_4$ .<sup>26,31</sup> Double salts with varying Ni and Co concentrations were studied using an equivalent  $(\text{NH}_4)_2\text{SO}_4$  concentration at room temperature. The resulting double salts show a preference of Ni over Co with Ni concentrations at nearly 30 wt%. This data suggests that Ni and Co could be further separated by fractional precipitation.<sup>28</sup> Three surrogate solutions that resemble LIBBM leachate were investigated that were Ni-rich, Co-rich, and 1 : 1 Ni/Co, all containing Li, Ni, Co and Mn without Cu, Fe, and Al. Experiments focused on changes in pH and the difference in concentrations of  $(\text{NH}_4)_2\text{SO}_4$ . The results showed that at a pH range from 1 to 5, there was little effect on Tutton's salt formation, and only

a minor separation between the Ni and Co percentages was observed, except for Mn at pH > 4. The data also showed little inclusion of Li in the Tutton's salt, which suggested Li would remain in solution. This conclusion agrees with our observations in Tutton's salt formation and fits in with the modelling data in this study. Furthermore, the modelling data shows that  $(\text{NH}_4)_2\text{SO}_4$  concentration is the key to drive Tutton's salt formation. At concentrations of 1.5 mol ammonium per mol metal, peak metal recovery of Ni and Co can be achieved which limits Mn and Li into the Tutton's salt. This separation is important because it should allow the isolation of Ni and Co from a mixed metal solution that includes Mn and Li, and the

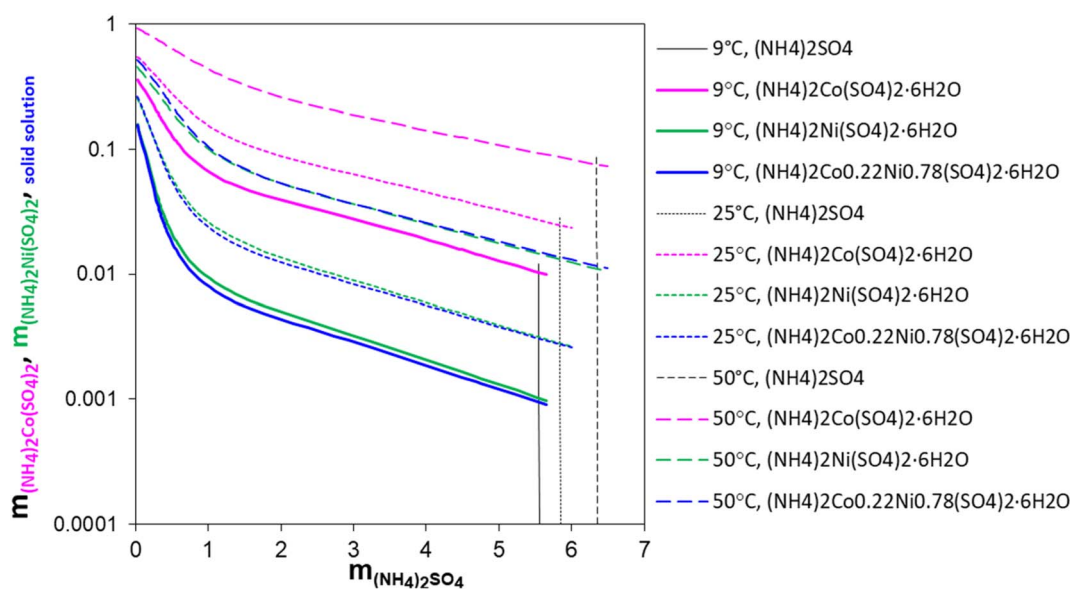


Fig. 4 Variation in calculated solubility of  $(\text{NH}_4)_2\text{Co}(\text{SO}_4)_2 \cdot 6\text{H}_2\text{O}$ ,  $(\text{NH}_4)_2\text{Ni}(\text{SO}_4)_2 \cdot 6\text{H}_2\text{O}$ , and Ni/Co Tutton's salt (referred to as solid solution, isolated  $(\text{NH}_4)_2\text{Co}_{0.22}\text{Ni}_{0.78}(\text{SO}_4)_2 \cdot 6\text{H}_2\text{O}$ ) in water as a function of added  $(\text{NH}_4)_2\text{SO}_4$  at 9 °C, 25 °C and 50 °C. Vertical black lines show the solubility of  $(\text{NH}_4)_2\text{SO}_4$  in this system at the specified temperatures. Unit: mol salt per kg water.



pH and Li concentration of the solution do not interfere with isolation of Ni and Co. Another factor to consider is temperature, which should allow better control over the sulfate double salt compositions, especially between Ni and Co that will be discussed later. From this standpoint, fractional precipitation should be possible to enrich Ni further from mixed metal EC-leach solutions.

### 3.4 Crystallization of Tutton's salts from surrogate solutions

A surrogate study was done to better understand Tutton's salts growth from complex solutions, such as EC-leachate, under controlled conditions including mother solution composition, temperature, and  $(\text{NH}_4)_2\text{SO}_4$  concentration after the phosphate impurity metal removal.<sup>16</sup> EC-leachates can have varied concentrations of Ni and Co depending on the types of cathodes. The separation method proposed in this article can effectively remove 99% of the Al and Fe by DAP and  $\text{NH}_4\text{OH}$  at pH 4; however, the efficiency of the process can be impacted by residual DAP, which may cause additional loss as precipitates or interference with the desired metals in the solution.

Previous data shows that the added phosphate is not fully consumed in Fe/Al precipitation, and the concentration of remaining phosphate in the solution will be about 7–12  $\text{mg mL}^{-1}$ .<sup>16</sup> This phosphate concentration was applied to the surrogate solutions. Small amounts of phosphate did not appear to affect the crystallization of the Tutton's salt. In addition, the solubility of Ni or Co phosphate salts are much higher than those of Al and Fe, which means that the remaining phosphate does not favor Ni or Co phosphate formation as a precipitate.

Temperature is another parameter in these crystallizations. From the thermodynamic modelling results, cooling these solutions should increase the yield of Tutton's salt formation. It is predicted that controlling the temperature during crystallization will change the Ni and Co composition of the Tutton's salt. If a higher composition of one element, especially Ni, can be achieved at a higher temperature during the Tutton's salt formation, then it should result in increased Co composition at lower temperatures. These variations in these surrogate solutions are pivotal in assisting further separations of Ni and Co.

To complete the series, the concentration of  $(\text{NH}_4)_2\text{SO}_4$  along with the concentrations of  $\text{NiSO}_4$  and  $\text{CoSO}_4$  from 0–100% were studied due to the possible combinations from recycled battery cathode materials. For the crystallization process, not only do we want to maximize our Ni and Co recovery, but also fractionally separate Co and Ni, which is indicated by the thermodynamic modelling results. Thus, a series of 1 and 1.5 molar ratios of  $(\text{NH}_4)_2\text{SO}_4$  to Ni and Co were prepared to study the effect of  $(\text{NH}_4)_2\text{SO}_4$  concentration on Ni and Co recovery.

A series of surrogate solutions were prepared with constant Mn and Li concentrations at 6  $\text{g L}^{-1}$  and 4  $\text{g L}^{-1}$ , respectively, and Ni and Co at a total concentration of 40  $\text{g L}^{-1}$ , with a Ni/Co wt% ratio ranging from 0–100% in 10% intervals. To simulate the phosphate precipitation, each surrogate solution was adjusted to pH 3 with DAP and to 4 with  $\text{NH}_4\text{OH}$ . A 2 M  $(\text{NH}_4)_2\text{SO}_4$  solution was mixed with the surrogate solutions at 40–50 °C, to prevent precipitation of the  $(\text{NH}_4)_2\text{SO}_4$  salt. The

amount of  $(\text{NH}_4)_2\text{SO}_4$  solution was based on two sets of 1 and 1.5 molar ratios to the combined Ni and Co. The solution then was split into two fractions that were stored at either room temperature (around 20 °C) or in a refrigerator at around 9 °C. After approximately 15 hours, crystals were observed at both temperatures. Solutions with higher Ni content appear green as did the precipitate, while solutions with more Co content were red in color. A spectrum between green and red for these crystals (see ESI S1†) indicates that Co-rich and Ni-rich Tutton's salts are not entirely different in the crystal structure. Most of the isolated crystals are fairly large and well defined, except those formed from at higher Ni content which appeared more granular. This effect is likely due to the solubility of the Ni sulfate double salts at higher Ni concentrations.

### 3.5 Metal composition in Tutton's salts from surrogate solutions

A crucial point with the Tutton's salt is the six water molecules in the crystal. As the sulfate double salts form, the metals in the leachates will also concentrate as water is incorporated into the crystal lattice. The surrogate solutions were kept at 50  $\text{g L}^{-1}$  total metal concentration for these experiments. Due to decreasing water volume and the wet salts isolated from the surrogate solutions, obtaining an accurate yield based on weight was challenging. However, to address this issue, the elemental composition of the precipitated crystals was compared to the initial leachate concentrations. Fig. 5 is a comparison of metal compositions in the crystals *versus* the Ni:Co atomic percent (at%) ratio in the surrogate mother solution. It shows a linear relationship with a slope nearly 1 between the composition of Ni or Co for the crystals compared to the parent solutions. Furthermore, no noticeable differences were observed between Ni and Co crystallization at different temperatures or  $(\text{NH}_4)_2\text{SO}_4$  concentration. However, crystallization at room temperature showed a higher Ni composition over Co in the crystals, which supports previous data indicating a preference for Ni over Co in the Tutton's salt crystals. For all concentrations and temperatures, Mn comprised of 0.5–1.25 at% in the Tutton's salt with a higher Mn content at higher concentrations of  $(\text{NH}_4)_2\text{SO}_4$  and lower temperature. Lastly, Li was observed in all the crystals, but most are less than 1 at%. However, this Li is considered a contaminant imparted from the mother liquor and not a part of the crystalline phase.

### 3.6 Percent metal recovery in Tutton's salts

In Fig. 6, the recovery of Ni and Co in the Tutton's salts reveals a similar trend that more metals (including Mn) could be incorporated into the crystals at high sulfate concentrations and a lower temperature. At both temperatures, over 70 wt% of Ni was removed from the surrogate mother solution regardless of the initial Ni concentration at room temperature, whereas over 90 wt% of Ni could be recovered at 9 °C and higher  $(\text{NH}_4)_2\text{SO}_4$  concentration. Between 30–80 wt% of Co was recovered in the double salts with higher  $(\text{NH}_4)_2\text{SO}_4$  concentration and lower temperature, but it also was dependent on the Ni concentration in the surrogate mother solution. This data



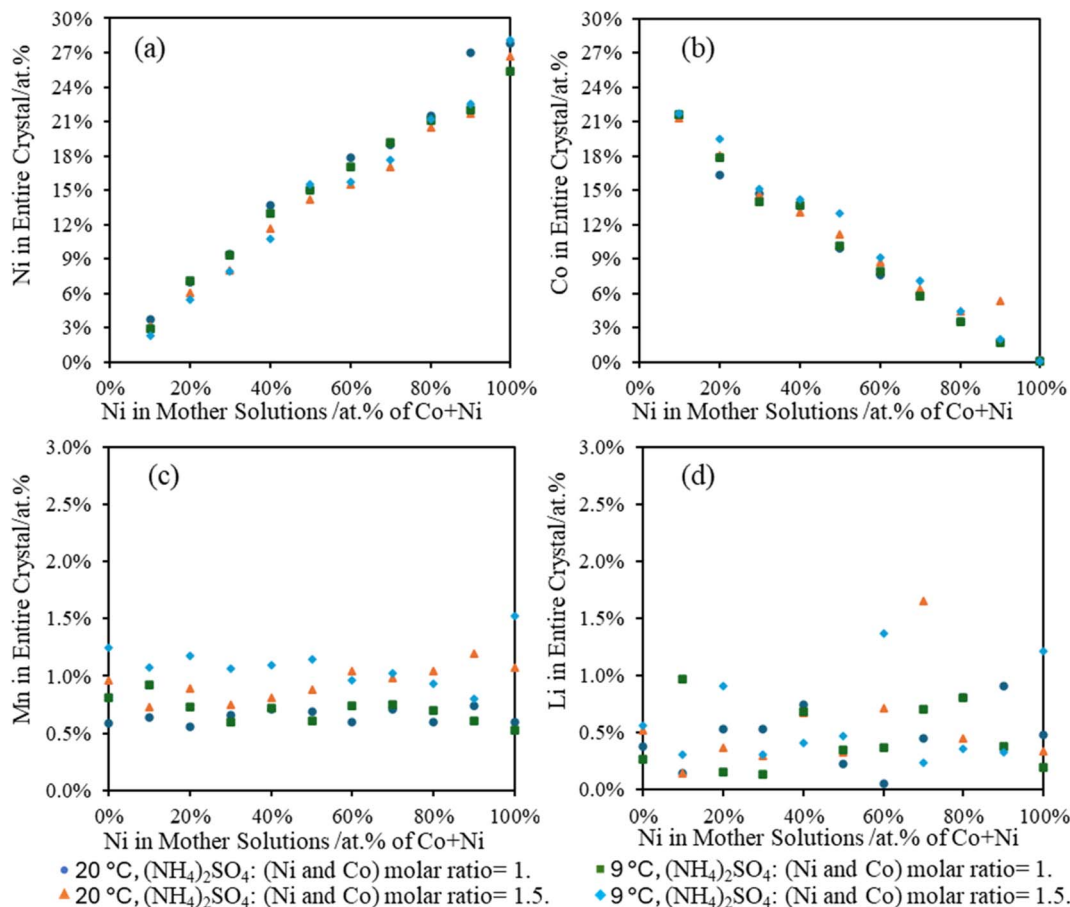


Fig. 5 Compositions of metal in the crystals formed in the surrogate mother solutions under different conditions: (a) Ni at% in crystals, (b) Co at% in crystals, (c) Mn at% in crystals, and (d) Li at% in crystals. Temperature: 9 °C and 20 °C. (NH<sub>4</sub>)<sub>2</sub>SO<sub>4</sub>: (Ni and Co) molar ratio = 1 and 1.5.

reveals that Co sulfate double salt formation is directly influenced by the Ni concentration; therefore, temperature and ammonium salt concentration can be utilized for fractional precipitation to increase Ni content over Co in the sulfate double salts.

From the various metal compositions in the surrogate mother solutions, the Li and Mn were found at lower concentrations in the isolated Tutton's salts. Between 10–40 wt% of Mn was observed in the Tutton's salts, where higher percentages of Mn were incorporated with increasing Ni compositions; however, less than 5 wt% Li precipitated out with the crystals. Overall, the formation of Tutton's salts from the EC-leachate can effectively recover over 70 wt% of Ni and Co, while the majority of the Mn and Li will remain in the leachate solutions.

### 3.7 Fractional crystallization – enrichment of Ni and Co from processed LIBBM EC-leach solution

The surrogate experiments and thermodynamic modelling data suggest that it is possible to remove and separate Ni and Co from EC-leachates where temperature is a major factor influencing Tutton's salt crystallization from solution. The Ni double salts are noticeably less soluble at room temperature compared to the Co double salts as observed from the surrogate experiments. To test an actual LIBBM leachate solution, we conducted

a series of EC-leach runs with impurity precipitation and the Tutton's salt recovery as shown in Fig. 7. It is noteworthy that over 70 wt% of Ni and Co from LIBBM could be isolated, without the need for any other metal or column extraction (SX or IX) technique.

Initially, EC-leach yielded a process solution after 19.5 hours. From 500 grams of LIBBM, a 1740 mL leachate volume was obtained with a  $\sim 71 \text{ g L}^{-1}$  ( $71\,028 \text{ mg L}^{-1}$ ) metal concentration at a final pH of 2.12 (Table 4(a)). LIBBM is a composite of cathode and anode materials, containing finer particles (millimeter and less) of carbon graphite, Cu and Al foil, electrolytes, and polymer separators. Most of the Cu was removed by electroplating at the cathode during EC-leach, and then the carbon graphite (and any other particulates) was filtered from the leachate to give a clear solution of metal ions. The leachate solution contains greater than  $20 \text{ g L}^{-1}$  for Co and Ni, as well as  $133 \text{ mg L}^{-1}$  Cu. After analyzing the metals in the EC-leachate black mass, the recovery efficiency was found to be slightly lower than surrogate experiments, which may be a result of slower reaction kinetics at a higher pH value. In this case, leaching efficiency of Li, Mn, and Ni were just over 85%, and that of Co was lower at 77%. Overall, the processed LIBBM leachate was Co-rich compared to Ni and Mn.



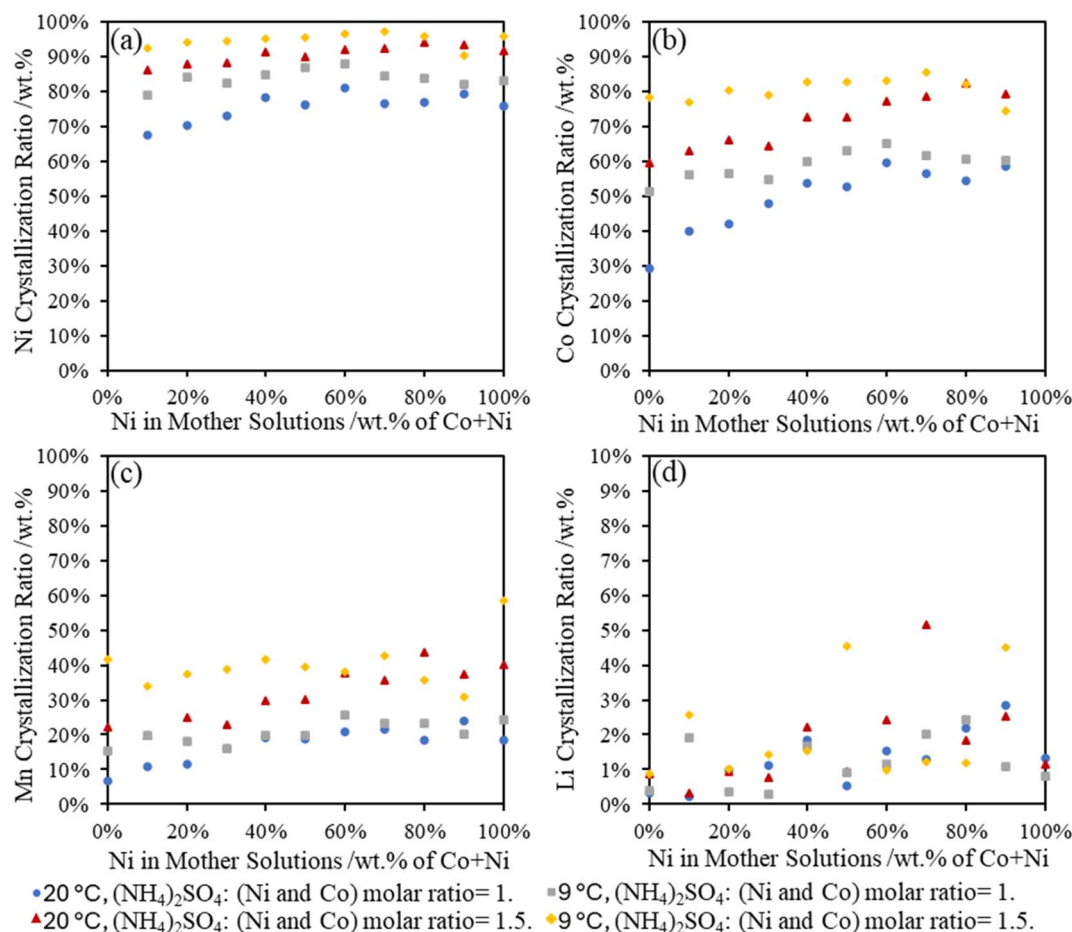


Fig. 6 Percentages of metal isolated in Tutton's salt under different conditions: (a) Ni wt% in crystals, (b) Co wt% in crystals, (c) Mn wt% in crystals, and (d) Li wt% in crystals. Temperature: 9 °C and 20 °C. (NH<sub>4</sub>)<sub>2</sub>SO<sub>4</sub>: (Ni and Co) molar ratio = 1 and 1.5.

Next in Fig. 7, the interference metal impurities (Al, Fe and Zn) were removed. Based on the amount of Fe in solution, H<sub>2</sub>O<sub>2</sub> was added per half mole of Fe to guarantee full oxidation to Fe(III). DAP was added to the heated leachate (45–50 °C) to increase the solution pH to 3 and then NH<sub>4</sub>OH was added to pH 4. Since the initial pH was 2.12, less DAP was needed to adjust pH to 3, and no precipitation of Tutton's salts were observed in the EC-leachate. In this experiment, ~0.017 g mL<sup>-1</sup> of DAP was

mixed into the leachate, and about 12 mL of 28–30 wt% NH<sub>4</sub>OH to achieve pH 4. Almost all Al and Fe were removed from the leachate as well as half of the Zn (see Table 4(b)). Around 10% loss was found in all desired critical metals (Li, Mn, Co, and Ni) during the impurity removal process. High concentrations of Li, Mn, Co, and Ni (~64 g L<sup>-1</sup>) remained in 1580 mL filtered clean leachate which was used in the next step.

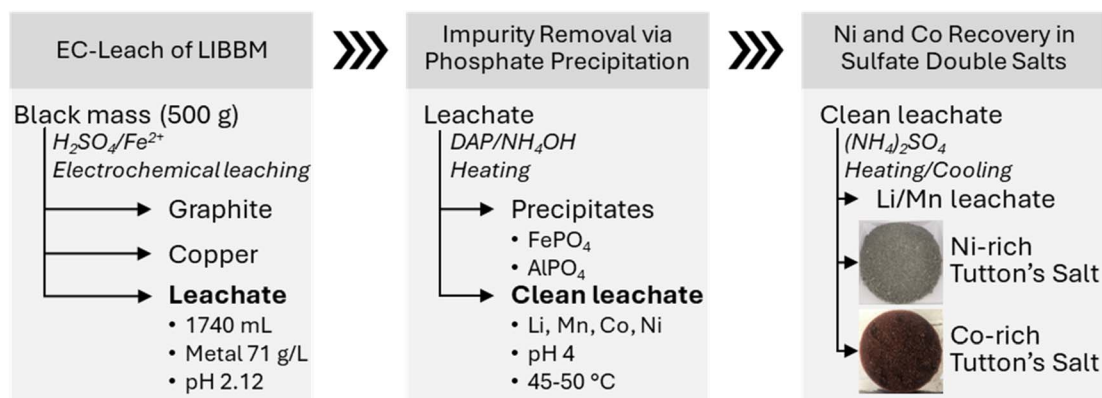


Fig. 7 LIBBM processing through three steps on the same leachate solution.



**Table 4** Metal compositions of (a) the EC-leachate from LIBBM, (b) clean leachate after phosphate precipitation, and (c) double salts and final processed filtration after crystallization

		Li	Cu	Al	Mn	Fe	Co	Ni	Cd	Zn
(a)	EC-leachate (mg L <sup>-1</sup> )	7017.6	132.6	1345.6	11 726.1	1664.8	27 482.8	21 453.2	9.9	193.9
	Leaching efficiency	87.7%	97.6%	85.0%	85.1%	60.5%	76.7%	86.7%	100.0%	95.6%
(b)	Clean leachate (mg L <sup>-1</sup> )	6506.7	78.5	0.0	10 470.9	7.5	25 381.9	21 753.5	6.7	109.0
	Precipitate ratio	9.7%	37.2%	100.0%	12.7%	99.6%	10.0%	9.2%	28.9%	46.6%
(c)	Final filtration (mg L <sup>-1</sup> )	8236.7	37.8	40.0	9006.9	3.5	4177.3	382.4	9.6	17.4
	First/Green crystal yield	2.8%	0.0%	23.1%	6.8%	27.4%	31.6%	62.5%	17.8%	31.8%
	Second/Red crystal yield	2.3%	29.7%	71.5%	30.1%	66.7%	57.1%	36.2%	41.4%	59.7%
	Entire crystal yield	5.1%	29.7%	94.6%	36.9%	94.1%	88.7%	98.7%	59.2%	91.5%
	First crystal composition	0.1%	0.0%	0.1%	0.5%	0.0%	5.5%	8.8%	0.0%	0.0%
	Second crystal composition	0.1%	0.0%	0.2%	1.6%	0.0%	7.8%	3.9%	0.0%	0.0%

In final step in Fig. 7, the processed leachate was heated to 70 °C and 283 g (NH<sub>4</sub>)<sub>2</sub>SO<sub>4</sub> was added, which resulted in a 1.5 : 1 molar ratio of sulfate to combined Co and Ni. The (NH<sub>4</sub>)<sub>2</sub>SO<sub>4</sub> dissolved rapidly as it was added until the solution reached a molar ratio of 1 : 1. Above this amount of (NH<sub>4</sub>)<sub>2</sub>SO<sub>4</sub>, green crystal precipitates began to form and suspend in the solution while stirring. Once the molar ratio reached 1.5 : 1 mole, the green precipitates were allowed to settle. The supernatant dark pink in color was poured into another flask and the green crystals were collected and dried at room temperature. Following refrigeration of the supernatant at 9 °C, red crystals grew at the bottom of the container overnight. Afterwards, the red crystals were collected and dried. Both of the collected Ni-rich and Co-rich Tutton's salts, as well as the remaining supernatant above the red crystals, were analyzed for metal ion concentration (Table 4(c)).

After the two crystallizations, the remaining supernatant volume was reduced by over 30%, and it remained optically clear with a light pink color. The Co concentration decreased from 25.4 g L<sup>-1</sup> to 4.2 g L<sup>-1</sup> upon the second precipitation. Ni also showed a dramatic concentration drop, from 21.8 g L<sup>-1</sup> to only 0.4 g L<sup>-1</sup>. For fractional crystallization, these two metals were effectively recovered in this two-stage crystallization.

For the first crystallization, 62.5% of Ni and 31.6% of Co from the parent solution were isolated as green crystals. For the second crystallization, an additional 36.2% of Ni and 57.1% Co were recovered in the red crystal compared to the starting EC-leachate solution. After this two-stage fractional crystallization, an estimated ~89% of Co and ~99% of Ni was retrieved from the starting EC-leachate solution. The overall time needed to complete the following processes was about 48 hours from the LIBBM to the isolated Ni-enriched and Co-enriched double salts.

From these isolated double salts, two other metals were observed in the red and green crystals. 2.8% Li and 6.8% Mn were calculated from the green crystals and 2.3% Li and 30.1% Mn were calculated from the red crystals. A total of 5.1% Li and 36.9% Mn were observed in the combined batches of crystals. As a result, the green crystals were Ni-enriched with a Ni to Co ratio of 3 : 2, whereas the red crystals were Co-enriched with a Co to Ni ratio of 2 : 1. The data for the metal balance from the starting EC-leachate concentration to isolated Tutton's salt concentrations were in good agreement with each other; however, Al, Cu,

Zn, Cd, and Fe was observed in the products which could be the result of contamination during the workup procedures. The most interesting feature of the isolated red and green crystals is that >99% of Ni, Co, Mn, and Li are the only metals observed from a large mixture of metals in the leachate. Although Ni and Co are not completely purified by these steps, this method using sulfate double salts can provide a quick pathway to enhance other enrichment processes, such as SX, IX, and electrowinning. The real potential value of this process would increase if it were possible to directly create new cathodic materials with the Ni-enriched salts, but this most likely would require little variability in spent LIBBM materials. However, if possible, this process could reduce the time and chemicals necessary to regenerate new cathodes.

## 4 Conclusion

A new hydrometallurgical method has been developed at the laboratory scale to isolate Co and Ni from LIBBM in three steps: (1) EC-leach, (2) DAP impurity metals precipitation, and (3) Tutton's salt crystallization. As a promising result, impurity metals (Al and Fe) are removed as their phosphates, and then the Ni-enriched and Co-enriched double salts are isolated from the remaining solution by crystallization. With this method, high-value products (sulfate salts) can be produced without additional separation methods, such as IX and SX, to isolate the Ni and Co from the solution. Although these two methodologies of impurity phosphate precipitation and Ni/Co double salt crystallization are described separately in the literature, the combination of these two into a single process for fractional precipitation has not been previously attempted.

From a NMC LIBBM containing nearly 2 : 1 : 2 composition ratio of Ni : Mn : Co, ~99% of impurity metals were removed as their phosphates, and then 99% of Ni and 89% of Co were isolated as their Tutton's salts. The caveat to the production of these double salts is co-crystallization of Mn. However, Mn sulfate double salt is more soluble than those with Co and Ni (*cf.*, ESI S2†), indicating that in the obtained Tutton's salt, Mn content will be less than that of Ni and Co. It is interesting that Ni, Co, and Mn dominate these crystals with only a small amount of entrained Li found. Taken together, this data suggests that Ni and Co can be quickly isolated from a leachate solution.



An enabling aspect of this process is the use of differing solubility limits between phosphate and sulfate in the EC-leachate solutions, which allow for facile Ni and Co separation. This process allows a simple Ni and Co separation after removing the impurity phosphates and then precipitating Ni and Co, as Tutton's salts, by adding more  $(\text{NH}_4)_2\text{SO}_4$ . As a result, no other separations methods, such as SX or IX, are necessary to recover high concentrations of Ni and Co double salts from the EC-leach, which means no organic solvents or additional extractants are required to isolate these metals. Another interesting aspect of this chemistry is the possibility of reusing the isolated Tutton's salts to generate battery cathode materials, which can reduce the dependence on non-domestic critical metal sources.

## Data availability

The data supporting this article have been included as part of the ESI.† Crystallographic data for **1** has been deposited at the CCDC under CSD 2361136. The code for thermodynamic model has been constructed using the Mixed-Solvent Electrolyte (MSE) framework can be found at DOI: [https://doi.org/10.1016/S0378-3812\(02\)00178-4](https://doi.org/10.1016/S0378-3812(02)00178-4) and <https://doi.org/10.1016/j.molliq.2005.11.030>.

## Conflicts of interest

There are no conflicts to declare.

## Acknowledgements

This work was supported by the Critical Materials Institute, an Energy Innovation Hub funded by the US Department of Energy, Office of Energy Efficiency and Renewable Energy, Advanced Materials and Manufacturing Technologies Office under Grant AL-12-350-001. The work at Idaho National Laboratory was conducted under contract DE-AC07-05ID14517. We would like to thank Richard Schutte and Anthony Rogers from Cirba Solutions for providing LIBBM from their recycling center.

## References

- 1 T. Or, S. W. D. Gourley, K. Kaliyappan, A. Yu and Z. Chen, Recycling of mixed cathode lithium-ion batteries for electric vehicles: Current status and future outlook, *Carbon Energy*, 2020, **2**, 6–43.
- 2 G. Harper, R. Sommerville, E. Kendrick, L. Driscoll, P. Slater, R. Stolkin, A. Walton, P. Christensen, O. Heidrich, S. Lambert, A. Abbott, K. Ryder, L. Gaines and P. Anderson, Recycling lithium-ion batteries from electric vehicles, *Nature*, 2019, **575**, 75–86.
- 3 Y. Li, W. Lv, H. Huang, W. Yan, X. Li, P. Ning, H. Cao and Z. Sun, Recycling of spent lithium-ion batteries in view of green chemistry, *Green Chem.*, 2021, **23**, 6139–6171.
- 4 A. B. Botelho Junior, D. B. Dreisinger and D. C. R. Espinosa, A Review of Nickel, Copper, and Cobalt Recovery by Chelating Ion Exchange Resins from Mining Processes and Mining Tailings, *Min., Metall., Explor.*, 2019, **36**, 199–213.
- 5 Y. Yao, M. Zhu, Z. Zhao, B. Tong, Y. Fan and Z. Hua, Hydrometallurgical Processes for Recycling Spent Lithium-Ion Batteries: A Critical Review, *ACS Sustainable Chem. Eng.*, 2018, **6**, 13611–13627.
- 6 G. S. Shyam Sunder, S. Adhikari, A. Rohanifar, A. Poudel and J. R. Kirchoff, Evolution of Environmentally Friendly Strategies for Metal Extraction, *Separations*, 2020, **7**, 4.
- 7 V. Innocenzi, N. M. Ippolito, I. De Michelis, M. Prisciandaro, F. Medici and F. Vegliò, A review of the processes and lab-scale techniques for the treatment of spent rechargeable NiMH batteries, *J. Power Sources*, 2017, **362**, 202–218.
- 8 L. A. Cisternas, C. M. Vásquez and R. E. Swaney, On the design of crystallization-based separation processes: Review and extension, *AIChE J.*, 2006, **52**, 1754–1769.
- 9 H. Bae and Y. Kim, Technologies of lithium recycling from waste lithium ion batteries: a review, *Mater. Adv.*, 2021, **2**, 3234–3250.
- 10 L. Brückner, J. Frank and T. Elwert, Industrial Recycling of Lithium-Ion Batteries—A Critical Review of Metallurgical Process Routes, *Metals*, 2020, **10**, 1107.
- 11 W. Lv, Z. Wang, H. Cao, Y. Sun, Y. Zhang and Z. Sun, A Critical Review and Analysis on the Recycling of Spent Lithium-Ion Batteries, *ACS Sustainable Chem. Eng.*, 2018, **6**, 1504–1521.
- 12 Pa Ho Hsu, Comparison of iron(III) and aluminum in precipitation of phosphate from solution, *Water Res.*, 1976, **10**, 903–907.
- 13 S. C. Chang and M. L. Jackson, Solubility Product of Iron Phosphate, *Soil Sci. Soc. Am. J.*, 1957, **21**, 265–269.
- 14 J. C. Brosheer, F. A. Lenfesty and J. F. Anderson, Solubility in the System Aluminum Phosphate-Phosphoric Acid-Water, *J. Am. Chem. Soc.*, 1954, **76**, 5951–5956.
- 15 L. A. Diaz, M. L. Strauss, B. Adhikari, J. R. Klaehn, J. S. McNally and T. E. Lister, Electrochemical-assisted leaching of active materials from lithium ion batteries, *Resour., Conserv. Recycl.*, 2020, **161**, 104900.
- 16 J. R. Klaehn, M. Shi, L. A. Diaz, D. E. Molina, S. M. Reich, O. Palasyuk, R. Repukaiti and T. E. Lister, Removal of impurity Metals as Phosphates from Lithium-ion Battery leachates, *Hydrometallurgy*, 2023, **217**, 106041.
- 17 G. M. Sheldrick, Crystal structure refinement with SHELXL, *Acta Crystallogr., Sect. C: Struct. Chem.*, 2015, **71**, 3–8.
- 18 P. Wang, A. Anderko and R. D. Young, A speciation-based model for mixed-solvent electrolyte systems, *Fluid Phase Equilib.*, 2002, **203**, 141–176.
- 19 P. Wang, A. Anderko, R. D. Springer and R. D. Young, Modeling phase equilibria and speciation in mixed-solvent electrolyte systems: II. Liquid-liquid equilibria and properties of associating electrolyte solutions, *J. Mol. Liq.*, 2006, **125**, 37–44.
- 20 M. S. Gruszkiewicz, D. A. Palmer, R. D. Springer, P. Wang and A. Anderko, Phase Behavior of Aqueous Na–K–Mg–Ca–Cl–NO<sub>3</sub> Mixtures: Isopiestic Measurements and Thermodynamic Modeling, *J. Solution Chem.*, 2007, **36**, 723–765.



- 21 G. Das, M. M. Lencka, A. Eslamimanesh, A. Anderko and R. E. Riman, Rare-earth elements in aqueous chloride systems: Thermodynamic modeling of binary and multicomponent systems in wide concentration ranges, *Fluid Phase Equilib.*, 2017, **452**, 16–57.
- 22 G. Das, M. M. Lencka, A. Eslamimanesh, P. Wang, A. Anderko, R. E. Riman and A. Navrotsky, Rare earth sulfates in aqueous systems: Thermodynamic modeling of binary and multicomponent systems over wide concentration and temperature ranges, *J. Chem. Thermodyn.*, 2019, **131**, 49–79.
- 23 P. Wang, A. Anderko, J. J. Kosinski, R. D. Springer and M. M. Lencka, Modeling Speciation and Solubility in Aqueous Systems Containing U(IV, VI), Np(IV, V, VI), Pu(III, IV, V, VI), Am(III), and Cm(III), *J. Solution Chem.*, 2017, **46**, 521–588.
- 24 P. Wang, A. Anderko, R. D. Springer, J. J. Kosinski and M. M. Lencka, Modeling chemical and phase equilibria in geochemical systems using a speciation-based model, *J. Geochem. Explor.*, 2010, **106**, 219–225.
- 25 A. Bejaoui, A. Souamti, M. Kahlaoui, A. D. Lozano-Gorrín, J. Morales Palomino and D. Ben Hassen Chehimi, Synthesis, characterization, thermal analysis and electrical properties of  $(\text{NH}_4)_2\text{M}(\text{SO}_4)_2 \cdot 6\text{H}_2\text{O}$  (M = Cu, Co, Ni), *Mater. Sci. Eng., B*, 2019, **240**, 97–105.
- 26 S. Ghosh, M. Oliveira, T. S. Pacheco, G. J. Perpétuo and C. J. Franco, Growth and characterization of ammonium nickel-cobalt sulfate Tutton's salt for UV light applications, *J. Cryst. Growth*, 2018, **487**, 104–115.
- 27 J. W. Mullin and M. M. Osman, Diffusivity, density, viscosity, and refractive index of nickel ammonium sulfate aqueous solutions, *J. Chem. Eng. Data*, 1967, **12**, 516–517.
- 28 A. Porvali, V. Agarwal, H. Angerla and M. Lundström, in *Ni-Co 2021: the 5th International Symposium on Nickel and Cobalt*, ed. C. Anderson, G. Goodall, S. Gostu, D. Gregurek, M. Lundström, C. Meskers, S. Nicol, E. Peuraniemi, F. Tesfaye, P. K. Tripathy, S. Wang and Y. Zhang, Springer International Publishing, 2021, pp. 81–89.
- 29 J. Slivnik, A. Rahten and D. Gantar, Study of Tutton's Salts  $(\text{NH}_4)_2\text{M}(\text{SO}_4)_2 \cdot 6\text{H}_2\text{O}$  with Mixed Metal Ions in the Structure, *Croat. Chem. Acta*, 1985, **58**, 289–294.
- 30 A. E. H. Tutton, I. The monoclinic double sulphates containing ammonium. Completion of the double sulphate series, *Philos. Trans. R. Soc., A*, 1916, **216**, 1–62.
- 31 M. de Oliveira, S. Ghosh, T. S. Pacheco, G. J. Perpétuo and C. J. Franco, Growth and structural analysis of ammonium nickel cobalt sulfate hexahydrate crystals, *Mater. Res. Express*, 2017, **4**, 105036.
- 32 L. A. Cisternas and D. F. Rudd, Process designs for fractional crystallization from solution, *Ind. Eng. Chem. Res.*, 1993, **32**, 1993–2005.
- 33 G. P. Demopoulos, Aqueous precipitation and crystallization for the production of particulate solids with desired properties, *Hydrometallurgy*, 2009, **96**, 199–214.
- 34 M. S. Moats and W. G. Davenport, in *Treatise on Process Metallurgy*, ed. S. Seetharaman, Elsevier, Boston, 2014, pp. 625–669.
- 35 C. Saal and A. C. Petereit, Optimizing solubility: Kinetic versus thermodynamic solubility temptations and risks, *Eur. J. Pharm. Sci.*, 2012, **47**, 589–595.
- 36 A. Benrath, Über die Polythermen der ternären Systeme, die neben Wasser je ein Sulfat der Alkalien und der Vitriolbildner enthalten. VI, *Z. für Anorg. Allg. Chem.*, 1932, **208**, 169–176.
- 37 R. M. Caven and W. K. Gardner, 221. Equilibria in the systems  $(\text{NH}_4)_2\text{SO}_4\text{-NiSO}_4\text{-H}_2\text{O}$ ,  $(\text{NH}_4)_2\text{SO}_4\text{-CoSO}_4\text{-H}_2\text{O}$ ,  $(\text{NH}_4)_2\text{SO}_4\text{-ZnSO}_4\text{-H}_2\text{O}$ ,  $\text{Na}_2\text{SO}_4\text{-NiSO}_4\text{-H}_2\text{O}$ , and  $\text{Na}_2\text{SO}_4\text{-CoSO}_4\text{-H}_2\text{O}$ , at 25°, *J. Chem. Soc.*, 1933, 943–946.
- 38 A. Fock, XX. Ueber die Löslichkeit von Mischkrystallen und die Grösse des Krystallmoleküls, *Z. Kristallogr. Cryst. Mater.*, 1897, **28**, 337–413.
- 39 A. E. Hill and W. J. Taylor Jr, Ternary Systems. XXIII. Solid Solution among the Picromerite Double Salts at 25°. The Zinc, Copper and Nickel Ammonium Sulfates, *J. Am. Chem. Soc.*, 1938, **60**, 1099–1104.
- 40 W. F. Linke and A. Seidell, Solubilities: inorganic and metal-organic compounds; a compilation of solubility data from the periodical literature. 2. K – Z, *Am. Chem. Soc.*, 1965, 255–453.
- 41 V. L. Manomenova, E. B. Rudneva, V. A. Komornikov, M. S. Lyasnikova, N. A. Vasilyeva and A. E. Voloshin, The ammonium cobalt sulfate hexahydrate (ACSH) crystal growth from aqueous solutions and some properties of solutions and crystals, *J. Cryst. Growth*, 2020, **532**, 125416.
- 42 A. Seidell, *Solubilities of Inorganic and Organic Substances: A Compilation of Quantitative Solubility Data from the Periodical Literature*, D. Van Nostrand Company, 1919.
- 43 G. Su, X. Zhuang, Y. He, Z. Li and G. Wang, Ammonium nickel sulfate hexahydrate crystal: a new ultraviolet light filter, *J. Phys. D: Appl. Phys.*, 2002, **35**, 2652.
- 44 G. Su, X. Zhuang, Y. He and G. Zheng, A new crystal of ammonium cobalt nickel sulfate hexahydrate for UV light band-pass filter, *Opt. Mater.*, 2008, **30**, 916–919.
- 45 Ed. Tobler, Ueber die Löslichkeit einiger schwefelsauren Salze der Magnesiareihe in Wasser, *Justus Liebigs Ann. Chem.*, 1855, **95**, 193–199.
- 46 C. R. v. Hauer, Ueber einige Salze, *J. Prakt. Chem.*, 1858, **74**, 431–436.
- 47 G. I. Gorshtein and N. I. Silant'yeva, The distribution of isomorphous and isodimorphous components between solid and liquid phases upon crystallization from aqueous solutions. III. Equilibrium in some systems containing double salts of the schoenite type, *Russ. J. Gen. Chem.*, 1954, **24**, 201–203.
- 48 B. Bertischówna, Contribution to the problem of solubility of mixed crystals, *Pol. J. Chem.*, 1926, **6**, 705–710.
- 49 J. Locke, The periodic system and the properties of inorganic compounds. IV. The solubility of double sulfates of the formula  $\text{MI}_2\text{MII}(\text{SO}_4)_2 \cdot 6\text{H}_2\text{O}$ , *Am. Chem. J.*, 1902, **27**, 455–481.
- 50 H. T. Kalmus and C. Harper, Physical Properties of the Metal Cobalt, *J. Ind. Eng. Chem.*, 1915, **7**, 6–17.

